

SGLDBench: A Benchmark Suite for Stress-Guided Lightweight 3D Designs

Junpeng Wang, Dennis R. Bukenberger, Simon Niedermayr, Christoph Neuhauser, Jun Wu, and Rüdiger Westermann

Abstract—We introduce the Stress-Guided Lightweight Design Benchmark (SGLDBench), a comprehensive benchmark suite to apply and evaluate material layout strategies for generating stiff lightweight designs in 3D domains. SGLDBench provides a seamlessly integrated simulation and analysis framework, providing six reference strategies accompanied by a scalable multigrid elasticity solver to efficiently execute these strategies and validate the stiffness of their results. This facilitates systematic analysis and comparison of design strategies regarding the mechanical properties they achieve. SGLDBench enables the evaluation of diverse settings of load conditions and, through the tight integration of the solver, enables support for high-resolution designs and stiffness analysis. Moreover, SGLDBench emphasizes visual analysis to explore relations between the geometric structure of a design and the distribution of stresses, providing insights into the specific properties and behaviors of different design strategies. SGLDBench's specific features are highlighted in several experiments, by comparing the results of reference strategies with respect to geometric and mechanical properties.

Index Terms—Topology optimization, lattice infill, lightweight design, simulation design.



1 INTRODUCTION

Topology optimization and functionally graded lattice infill are primary strategies for designing mechanically sound lightweight structures, i.e., structures with high stiffness when loaded via external forces. Topology optimization [1], [2] transforms the design process into an optimization problem of determining where to place material. Functionally graded lattice infill can be considered a rational distribution of lightweight (meta-)material with a geometric representation [3].

Topology optimization usually does not consider the geometric structure of the resulting material layout. Lattice infill, on the other hand, uses a structure made of individual edges (the struts), forming a graph or a grid composed of polyhedral cells (the scaffold). For designing load-bearing structures, tailoring the layout of lattice infill based on the stress distribution is key to achieving high structural performance. In particular, the structural rigidity of an infill is increased if the material is aligning with orthogonal principal stress directions in the object under load [4]. In the limit of material volume, this alignment forms micro-structures resembling quads or hexahedra [5].

Many different strategies for generating lightweight structures have been proposed over the last years [3], [12], [13], [14], the majority of them demonstrated on 2D domains. While the extension of topology optimization to 3D is rather straightforward, the generation of 3D-domain-filling lattice structures that follow the major stress directions is challenging. This is in particular due to the existence of degenerate points [15] (or degenerate regions in

3D domains [16], [17], [18]) where the stress tensor has repeating eigenvalues and the principal stress directions cannot be decided. Due to this, integrability conditions are violated and consistent domain parameterizations cannot be computed [19].

Topology optimization, in its basic form, aims at achieving the highest structural stiffness. In principle, alternative strategies share this goal, yet each has additional considerations that may come with a compromise in stiffness, such as achieving geometric properties like regularity (i.e., element type variation), uniformity (i.e., element size variation) or space-fillingness for improved robustness, as well as purely aesthetic features. To support users in selecting the best strategy for different use cases and researchers in identifying open research questions, a benchmark suite for generating, analyzing, and comparing the results of different strategies is required.

A few benchmark papers have addressed issues like special solvers for topology optimization [20], benchmarks for 2D topology optimization in specific load cases [21], practices that should be considered when performing topology optimization [22], as well as the mechanical soundness of simple lattice infills like orthogonal grids and shells [23]. Different architectures for multidisciplinary design optimization have been reviewed and compared [24], and issues of design and structural optimization of lightweight design have been discussed, especially in the context of additive manufacturing [12]. A review of uniform and non-uniform lattice structures such as foams and honeycombs sheds light on their properties and methods for designing and optimizing such structures [25], [26]. Unit cell lattices comprising structures made of a single type of cells have been researched [27], and the properties of certain types of lattice infills regarding 3D printing processes have been discussed [28]. The combination of topology optimization and micro element-based lattice infills have resulted in structures exhibiting anisotropic mechanical properties [29]. A benchmark enabling researchers and users to efficiently compute 3D designs with different strategies and effectively compare the results regarding their mechanical and structural properties does not exist.

- *J. Wang, D. Bukenberger, S. Niedermayr, C. Neuhauser and R. Westermann are with the Computer Graphics & Visualization Group, Technische Universität München, Garching, Germany.
E-mail: {junpeng.wang, dennis.bukenberger, simon.niedermayr, christoph.neuhauser, westermann}@tum.de.*
- *J. Wu is with the Department of Sustainable Design Engineering, Delft University of Technology, Delft, The Netherlands.
E-mail: j.wu-1@tudelft.nl.*

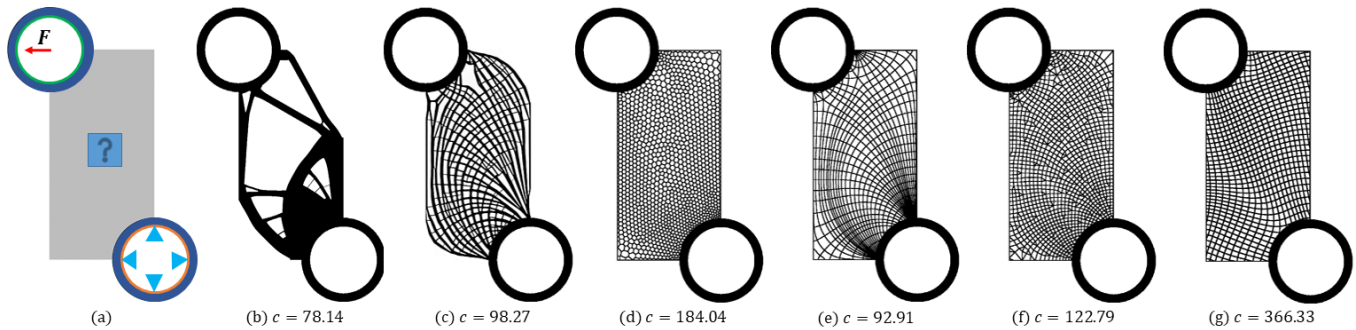


Fig. 1. Motivational example. (a) Problem description. The greyish region shows the design domain. Black rings indicate fully solid passive elements. A constant load exerts on all inner boundary vertices of the upper ring (green). All inner boundary vertices of the bottom ring (orange) are fixed. (b) density-based topology optimization [6]. (c) Porous infill optimization [7]. (d) Voronoi infill [8]. (e) Stress-line-guided material layout [9]. (f) Conforming lattice structures [10]. (g) Volumetric Michell trusses [11]. All designs consume roughly the same amount of material. c refers to the compliance of the design, which is measured by the strain energy.

We introduce *SGLDBench* to close this gap. It comprehensively investigates the combination of boundary shapes and conditions with lightweight design strategies in 3D domains. We demonstrate *SGLDBench* with reference strategies, including comparisons regarding mechanical and geometric properties. This is made possible by a seamlessly integrated, MATLAB-based simulation framework, which implements a number of reference strategies. To facilitate an effective comparison of different designs, *SGLDBench* generates a scalar material field regardless of the used strategy, and provides options to analyze the stiffness and structure of this field.

SGLDBench offers the following key features:

- **Selection of Lightweight 3D Design Strategies:** The benchmark offers different strategies that allow for drawing analogies between topology optimization and lattice infill, and enable comparative studies with new scenarios and designs.
- **Material Layout Generation:** Central to the benchmark is the voxelization of complex infills into a Cartesian simulation grid, to enable a consistent comparison of different lightweight designs—given as a material field, a mesh, or just an edge-graph—regarding their mechanical properties.
- **Simulation Suite:** *SGLDBench* provides a MATLAB-interfaced simulation framework including an efficient multigrid solver to generate high-resolution stress fields and efficiently assess the stiffness of a design.
- **Visual Design Analysis:** The benchmark is accompanied by a fast volume visualization module, providing visual feedback regarding a design’s shape, and the stress directions and material alignment before and after layout optimization.

We chose MATLAB as working environment due to its widespread use in computational design. *SGLDBench* utilizes MATLAB’s simulation and visualization operations for design generation and analysis. New design strategies can be integrated, either by MATLAB programs or by using MATLAB’s functionality to call executables or Python programs from other code bases via inline calls. All *SGLDBench* specific operations have been either implemented in MATLAB or are publicly available MATLAB or C++/Python programs. *SGLDBench* calls publicly available external libraries for core operations such as meshing and voxelization. The visualization module has been implemented in WebGL to enable its use either as a standalone viewer in a web-browser, or via inline calls to MATLAB’s viewing functionality. Upon acceptance, the entire code basis of *SGLDBench* will be made publically available.

2 FROM BOUNDARY CONDITIONS TO MATERIAL LAYOUTS

We first discuss a motivational study in 2D that illustrates several key aspects of *SGLDBench*. The user specifies the **boundary conditions**, i.e., the boundary of a domain as well as the exerting loads and fixed boundary parts, see Fig. 1a. The domain is then voxelized, i.e., it is discretized with a Cartesian grid, and per-voxel properties are set according to the boundary conditions and material properties. We call this configuration a **preset**.

With the selected preset, *SGLDBench* **simulates the object’s internal stress field** using a multigrid finite-element elasticity solver [30], [31], [32], [33]. While some design strategies require repeated solver executions to iteratively optimize the material layout, some others generate an infill structure that is guided by the principal stresses in the initial field.

The user can select from **six layout strategies** for computing an **infill design**: topology optimization [34], porous infill optimization [7], Voronoi infill [8], stress-line-guided material layout [9], conforming lattice structures [10] and volumetric Michell trusses [11].

Our selection has not been made with the intention to favor any of these methods, but to reveal the specific characteristics of 3D design strategies following different objectives. The methods span a wide spectrum from purely compliance-based optimization to geometry-aware infill generation. We select **density-based topology optimization** as representative of various topology optimization approaches. It serves as a reference for the compliance that can be achieved. **Porous infill optimization**, while not explicitly using the principal stress directions, results in wall-like structures that largely agree with two of these directions. **Voronoi infill** considers only the stress magnitude but not its principal directions. In contrast, material layouts guided by the **Principal Stress Lines (PSLs)** follow exactly the principal stress trajectories in the initial solid domain. PSL-guided infills serve as a reference conveying these directions, even though the final designs are not connected in general. **Conforming lattice structures** and **volumetric Michell trusses** aim at finding a balance between stress alignment and geometric regularity of the resulting designs. While the first approach favors stress alignment and, therefore, needs to resort to an edge-graph structure, the latter approach strives for a pure hexahedral mesh and, therefore, needs to sacrifice stress alignment. Figs. 1b-g show the infill designs computed by these methods with our motivational 2D example.

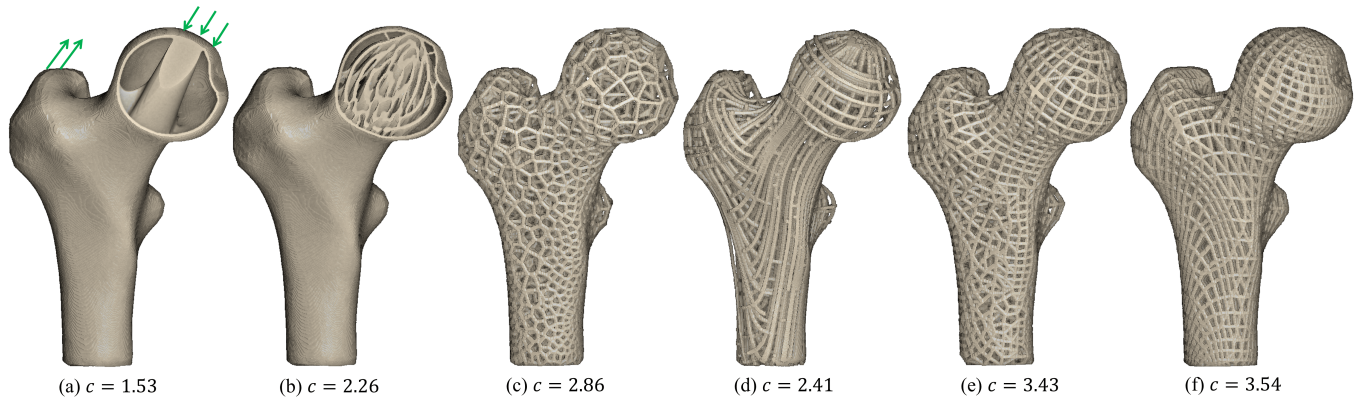


Fig. 2. Design strategies producing a 3D material field: (a) Density-based topology optimization [6]. (b) Porous infill optimization [7]. Design strategies producing a graph structure: (c) Voronoi infill [8]. (d) Stress-line-guided material layout [9]. (e) Conforming lattice structures [10]. (f) Volumetric Michell trusses [11]. All designs consume roughly the same volume fraction of 0.4, and they are subject to the same boundary conditions, i.e., the bottom of the design domain is fixed, and the loads are indicated by green arrows in (a). Below each design is its compliance. SGLDBench uses isosurface volume rendering with ambient occlusion for visualization. All designs are coated with fully solid boundary elements with a consistent thickness. In (c) to (f), these elements are peeled away to show the infills.

While topology optimization and porous infill generate a material field, all other methods compute a lattice structure composed of edges and nodes. SGLDBench can show lattice structures via MATLAB’s visualization functionality, by rendering edges as cylinders with a selected width. In addition, SGLDBench **voxelizes** each optimized lattice structure into a material field on a Cartesian grid with the same resolution as the initial preset. For a final material field and boundary conditions, the linear elasticity solver computes the **compliance of the design**, i.e., the inverse stiffness or strain energy. Notably, the user can also upload a material field and define a preset to perform the analysis with SGLDBench. Thus, the user can assess the robustness of a design with respect to loads it has not been optimized for.

SGLDBench supports different **visual analysis** options to inspect a 3D design. The geometry of a design is visualized via isosurface rendering of the 3D material field—in combination with a view-plane-aligned clip-plane—to convey a design’s uniformity and regularity. For a 3D human femur under load, Fig. 2 shows visualizations of the infill designs that are produced with SGLDBench’s methods, together with their compliances when loaded with the specific boundary forces. The compliance of each design reveals the relationship between stiffness and structure. The 3D stress fields produced by SGLDBench can be visualized with trajectory-based visualization techniques available in MATLAB [35]. Over that, SGLDBench provides tailored visualization options to investigate how the mechanical properties of the initial solid and the generated infill design change. Direct volume rendering is used with predefined color and opacity transfer functions to reveal the per-voxel deviation of the stresses in a final design from the stresses in the initial solid body (see Fig. 3).

3 COMPONENTS OF SGLDBENCH

We describe here the most important features and operations of SGLDBench, including descriptions of the supported topology optimization and lattice infill methods. The use of SGLDBench is demonstrated in the accompanying video.

3.1 Domain specification

SGLDBench simulates a stress field in the design domain using Finite Element Analysis (FEA). This requires discretizing the

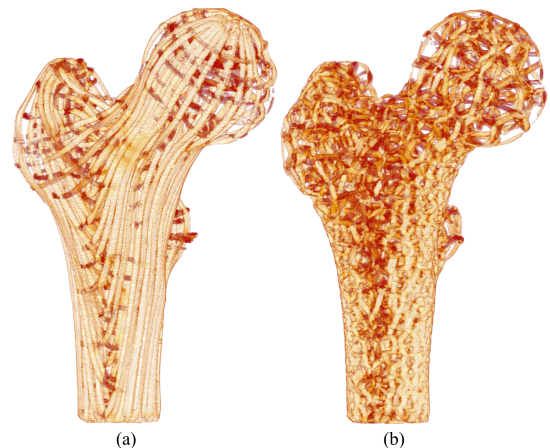


Fig. 3. Exemplary visual analysis of stresses in (a) a PSL-guided infill and (b) a Voronoi infill. Per voxel deviation between the major stress direction under the same load in the initial solid object and the infills is color-coded from light brown (low) to dark brown (high). The PSL-guided infill follows the initial stress directions and produces similarly directed stresses. Voronoi infill edges in the object interior are not related to the initial stress directions. Edges going through the passive boundary elements (which are the same in the solid and the voxelized infill) have approximately the same stresses.

domain into finite elements and specifying boundary conditions. SGLDBench uses a hexahedral finite-element representation to facilitate the use of scalable geometric multigrid solvers. Therefore, SGLDBench first converts an initial object representation to a hexahedral simulation grid.

Voxelization. The simulation grid is computed by voxelizing the simulation domain. The user inputs the domain boundary as a closed triangular mesh. SGLDBench uses MATLAB’s voxelization capabilities [36] with a user-defined voxel resolution to compute a solid voxelization. Alternatively, the user can upload a 3D voxel grid discretizing the domain and flagging each voxel representing the object as solid or void otherwise. All voxels with at least one exterior voxel in their 26-neighborhood are considered boundary voxels. SGLDBench provides a dilation operation to thicken the current boundary, setting each exterior voxel with at least one boundary voxel in its 26-neighborhood as boundary. The voxelized object is the basis of all subsequent operations in SGLDBench.

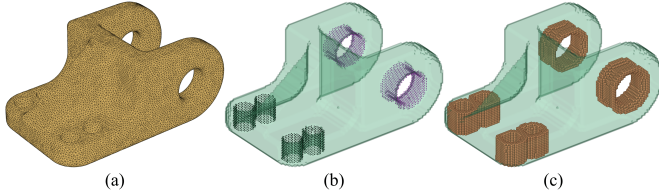


Fig. 4. From the design domain to the finite element model with boundary conditions. (a) A triangle mesh defines the domain boundary. (b) After voxelizing the domain, the user specifies boundary forces and fixations at grid vertices. Black and violet dots, respectively, indicate fixed vertices and vertices loaded with a constant downward force. (c) Passive elements are shown in brown.

Boundary Conditions. To conduct a linear elasticity simulation of an object using FEA, the boundary conditions need to be specified, i.e., where the object is fixed, and where and how the object is loaded. Fixations and forces are applied at nodes of the boundary elements. The user defines the extent and position of an axis-aligned box (or a sphere), and SGLDBench automatically fixes or assigns a specified load to all boundary nodes within this object. In the same way, the nodes which should be reset can be selected. When all nodes of a finite element are fixed, the entire element is fixed, i.e., it becomes rigid and does not respond to any loads.

Passive Elements. In many practical design and optimization scenarios, passive elements are used to maintain certain geometric features, like the object boundary or notches in a machine part where connections will be mounted. A passive element is constantly solid during design and optimization, and it contributes to the stiffness of the design. SGLDBench considers two general situations for specifying the passive elements. One is to set all boundary elements to passive, corresponding to a common infill design problem. Another one is to set the elements with loaded or fixed nodes to passive, to maintain certain prescribed features after design and optimization. By using a dilation operation, passive structures can be enlarged. Fig. 4 shows the transformation from a boundary mesh to a voxel model with boundary conditions and passive elements.

3.2 Stress simulation

At the core of topology optimization and lattice infill methods is the numerical simulation of a stress tensor field using the selected boundary conditions and material properties. SGLDBench provides a MATLAB-interfaced C++ implementation of a multigrid elasticity solver to efficiently simulate the stress field. The implementation uses a geometric multigrid solver as a preconditioner for a conjugate gradient method to solve a sparse linear system of equations, i.e., $KU = F$. The global stiffness matrix K is assembled from the element stiffness matrices under the assumption of a linear material law. The computation of the element stiffness matrices considers the stiffness tensor to reflect the material properties and the strain matrix to express the strain-stress relationship. U is the static displacement vector responding to the external loads F . A number of previous works have addressed the efficient assembly of the system matrix K as well as the specific adaptations of numerical solvers for linear elasticity simulation in the context of topology optimization [30], [31], [32], [33], [37].

SGLDBench’s multigrid implementation follows mostly the one by Wu et al. [31], in that it assembles numerical stencils on-the-fly and performs multigrid interpolation and restriction across multiple levels simultaneously. However, since the implementation is designed for MATLAB running on a CPU, some of the

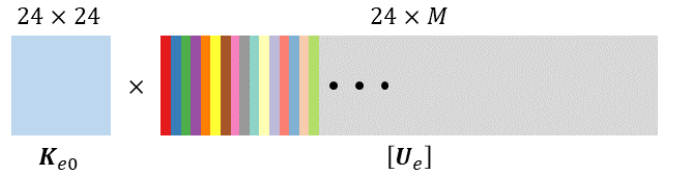


Fig. 5. Element-based computation layout. M is the number of hexahedral simulation elements, K_{e0} is the generic element stiffness matrix and U_e is the element-wise displacement matrix. Different colors represent the 8 node-based displacement vectors per element. With each column l_i in U_e , MATLAB computes the product $K_{e0} \cdot l_i$

internal data and computation layouts have been changed. Firstly, SGLDBench uses MATLAB’s built-in Cholesky solver instead of the Cholesky solver from the TAUCS library for solving the linear system on the coarsest multigrid level. Secondly, SGLDBench switches from a matrix-free node-based computation layout to a matrix-free element-based one to leverage MATLAB’s powerful matrix-vector operations. Instead of assembling the stencils per grid vertex on-the-fly via indexed memory access operations, SGLDBench builds a generic element matrix and uses MATLAB to efficiently compute the products of this matrix and the 8-node displacement vectors of each single element. Since the stiffness matrix of an element with density ρ is obtained by correspondingly scaling the generic stiffness matrix, the final results only need to be scaled by ρ . For each element, the 8 displacement vectors at the vertices are assembled into one column of an element-wise displacement matrix as shown in Fig. 5. MATLAB is then used to compute all matrix-vector products between the generic element matrix and each column in the displacement matrix.

3.3 Infill computation

For each of the six lightweight design methods provided by SGLDBench, the user selects specific parameters and lets SGLDBench compute the material layout. SGLDBench provides MATLAB code for topology optimization, porous infill optimization, PSL-guided material layout and volumetric Michell trusses. To generate a Voronoi infill, MATLAB calls a Python script including pre-compiled libraries. Conforming lattice structures are generated by compiling code from a publically available repository and running the executable from MATLAB with the required parameters.

3.3.1 Topology optimization

Topology optimization minimizes the compliance of a material layout under the constraint of exerting forces and a prescribed global material consumption. SGLDBench implements the density-based topology optimization approach [34], [38]. To formulate the minimization problem over a discrete set of elements e with pseudo densities ρ_e , a generated voxel model is used to build a hexahedral finite element discretization of a linear elastic material. The object’s compliance c is computed by summing the strain energy over all material elements, i.e.,

$$c = U^T K U. \quad (1)$$

The lower the compliance, the higher the object’s stiffness.

With selected material properties, i.e., Young’s modulus E_0 of the solid ($\rho_e = 1$) and the linear material law, topology optimization proceeds in three steps: 1) A large linear system is solved using the MATLAB multigrid implementation to compute the force-induced displacements of the hexahedral vertices. 2) The derivatives of the

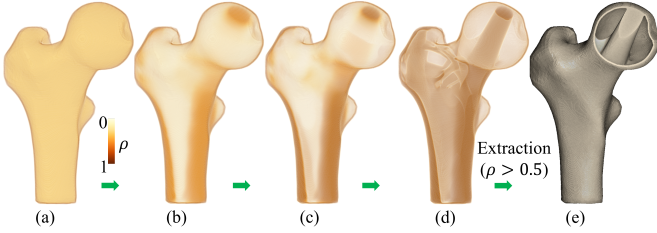


Fig. 6. Topology optimization process. (a) to (d): intermediate states of the optimized material field, with per voxel material fill-rate in $(0,1)$. (e) Final binary material field after thresholding.

total strain energy c and the total volume V with respect to the elements' material variables ρ_e are computed and used to guide the material distribution to maximize stiffness. 3) The design is updated according to the computed sensitivities. These steps are repeated until the change in material distribution is below a threshold or the number of iterations reaches the prescribed maximum iterations. The computational pipeline for topology optimization is mainly written in MATLAB, using optimized C++ code for solving the linear system and updating the design variables.

Density-based topology optimization takes the available material budget V_0 as the constraint, known as the global volume constraint. Thus, the problem-specific constraint function for a material layout ϕ using n hexahedral elements is

$$g(\phi) = \sum \rho_e - nV_0 \leq 0 \quad (2)$$

We use the so-called Solid Isotropic Material with Penalization (SIMP) model, where a non-zero constant minimum value represents the background stiffness of the void region. Topology optimization is conducted in an iterative manner. In each iteration, the design variables are updated within a prescribed step size through a gradient-based optimizer. SGLDBench uses the optimality criteria method to do so [34]. After optimization, the design variables shall converge to a (near-) binary layout that indicates the spatial material distribution.

It's worth mentioning that several auxiliary processes are also introduced in practical topology optimization for good design quality. For instance, the density-based filtering to counteract numerical instabilities and the Heaviside projection to promote the generation of a binary design, where the proxy density value of each voxel is encoded by the projected value of the filtered value of the design variable [39].

Fig. 6 shows the optimized shapes after different optimization iterations. The optimization produces a mono-scale design comprising mainly a thick resistant strand along the maximum stress directions.

3.3.2 Porous infill optimization

Porous infill optimization is an extension of density-based topology optimization. It creates porous substructures that spread across the design domain. This is achieved by replacing the global volume constraint with local volume constraints that prevent materials from accumulating and forming bold solid regions. Specifically, the global volume constraint restricts the total material consumption in the simulation domain. In contrast, the local volume constraint enforces an upper bound V_e for the percentage of solid voxels over all voxels in a prescribed neighborhood of voxel e . Apart from this, the optimization process follows mostly the one used by density-based topology optimization.

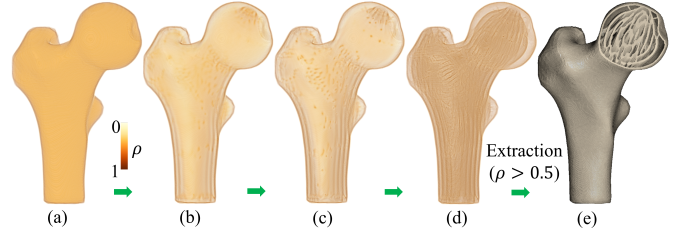


Fig. 7. Porous infill optimization process. (a) to (d): intermediate states of the optimized material field, with per voxel material fill-rate in $(0,1)$. (e) Final binary material field after thresholding.

For the material around at each voxel e , the local volume constraint leads to the constraint function

$$g(\phi_e) = \frac{\sum_{i \in N_e} \rho_i}{\sum_{i \in N_e} 1} - V_e \leq 0. \quad (3)$$

N_e defines the voxel neighborhood that is considered, i.e.,

$$N_e = \{i \mid \|x_i - x_e\|_2 \leq R_e\}, \forall e. \quad (4)$$

R_e is the radius of a spherical region centered at a voxel's center in which the local material accumulation is counted. SGLDBench's implementation of density-based topology optimization in MATLAB has been extended about the specific constraint function of porous infill optimization. The method of moving asymptotes (MMA) is used as the optimizer to update the design variables [40].

Fig. 7 shows the optimization process of porous infill optimization. In contrast to standard topology optimization, porous infill optimization produces a space-filling multi-scale design. Such designs show lower stiffness than those produced by topology optimization subject to a global volume constraint since some material is deposited in regions that do not contribute significantly to the overall stiffness. On the other hand, in general, such designs are more robust with respect to varying load conditions and local damage [7], [9]. Furthermore, porous infill optimization in 3D tends to form wall-like structures that are along the major and minor principal stress directions, see Fig. 2b.

3.3.3 Voronoi Infill

3D Voronoi infills are generated by computing an initial Delaunay tetrahedralization, based on a set of samples (S) following a stress-based distribution density. Therefore, more samples are generated in regions of higher stress, whereas the sampling density is lower in less stress-critical regions [8]. The Voronoi mesh follows as the dual of the Delaunay complex. Procedural infill optimization techniques building upon similar concepts have been proposed for additive manufacturing [41], [42].

Graded Sampling. In SGLDBench, S is initialized with a small set of auxiliary samples, equally distributed on a sphere, fully enclosing the input object. Further initial samples are added from the set of vertices of the input object's hull. Then, the input tetrahedral mesh is used as sampling domain, where S is iteratively updated in a progressive Poisson disk sampling scheme until no further samples can be added. For improved performance, this is realized using batches of n samples per iteration and organizing S in a kd-tree. Radii for Poisson disks are interpolated at their sample positions based on the von Mises stress field σ_{vm} , using the mapping

$$R = \text{icdf}(\sigma_{vm}) \cdot (\hat{r}\rho - \hat{r}) + \hat{r} \quad (5)$$

where \hat{r} the size of the largest radius (determined as a fraction of the objects bounding box diagonal length) and $\rho \in (0, 1]$ gives the

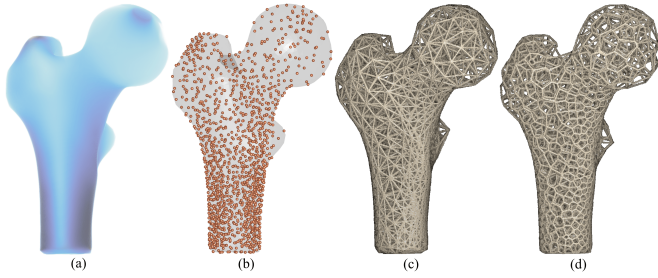


Fig. 8. Stress-aware Voronoi infill. (a) Scalar von Mises stress field. (b) Point cloud with stress-aware density. (c) Tetrahedral Delaunay mesh from (b). (d) Voronoi infill from (c).

ratio of smallest to largest radii. As the von Mises stress has an arbitrary range from smallest to largest values with spatially very concentrated extremes, we normalize and homogenize the field using an *inverse cumulative distribution function* (icdf).

Restricted Delaunay / Voronoi. The Delaunay complex or Voronoi diagram resulting from the generated samples are not natively limited to the design domain, i.e., the object’s outer boundary. As S includes vertices from the object’s hull as samples, the Delaunay complex is restricted to the object’s shape by simply excluding Delaunay simplices outside of the object using robust winding numbers [43]. Due to the dual nature of the Voronoi diagram and the Delaunay complex, the Voronoi cells of such hull vertex samples always transcend the object’s outer boundary. Therefore, Voronoi cells crossing the outer hull are cut and clipped [44], [45] such that only their inner part remains, cells fully outside are omitted.

As seen in Fig. 3, the edges of the Voronoi infill do not follow the direction of stresses in the initial solid object. Whereas the Delaunay criterion guarantees the most regular simplices when applied on the available sampling points, there is no trivial control for edge directions in the Voronoi graph, for instance, to construct Voronoi infills with controlled elasticity [41] or constraint alignment of the Voronoi edges [46].

SGLDBench provides Voronoi infill generation via Python due to the easy accessibility of required functionality. The SciPy [47] library is used to generate the Voronoi and Delaunay graphs using Qhull [48] and further provides the kd-tree acceleration structure for the Poisson disk sampling. Our code includes fallback methods required for restricting the graph structure to the object domain. See Fig. 8.

3.3.4 PSL-guided lattice infill

In the seminal work by Michell [5] on stiffness-optimal lightweight design, it was conjectured that a stiffness-optimal structure should bear only normal stresses. This means that the sub-structures of such a design align with the principal stress directions. This is known as *Michell’s Theory*, which has been considered since then in various lightweight design methods.

The most straightforward approach to create an infill that considers the principal stress directions in the loaded solid domain is to deposit material along the principal stress lines (PSLs), i.e., the mutually orthogonal trajectories following the major, minor, and medium eigendirections in the stress tensor field. When using line seeding strategies to obtain an as uniform as possible and domain filling distribution of PSLs [9], [49], PSL-guided infills show surprisingly good mechanical properties in 2D domains. In 3D domains, however, many PSLs do not significantly contribute to the infill’s stiffness, and PSLs might travel through space over a

long distance before they intersect with any other PSL or attach to the boundary (see Fig. 10a).

On the other hand, when performing material deposition by voxelizing lines with a selected thickness, the thicker the PSL trajectory is, the more connections are generated. This increases significantly the mechanical performance, and it often results in infills that show superior mechanical properties. In addition, since the stress field needs to be computed only once in the solid domain, the computational complexity is significantly reduced.

SGLDBench uses the publically available MATLAB backend of 3D-TSV [35] to generate PSLs in a 3D stress tensor field. The implemented method aims at producing a domain-filling and evenly-spaced set of PSLs. The method starts from a set of domain-filling seed points and iteratively creates PSL from these seeds. All remaining seeds in a certain distance to the PSL are removed to control the sparseness of the resulting PSL distribution. The thickness of PSLs is selected by the user, and for a selected thickness the density of seeded PSLs is iteratively increased until the given volume budget is roughly reached. A PSL might enter into a region where the three principal stress directions are not uniquely defined and exchange their orientation, i.e., around so-called degenerate points [15]. Tracing a PSL stops if the resulting directional change exceeds a given limit, and the PSL is removed to avoid wasting material.

3.3.5 Conforming lattice structure

Conforming lattice structure originates from the geometry-based structural dehomogenization presented by Wu *et al* [50]. In a general term, structural dehomogenization [51], [52], [53] diverges from the fine-resolution simulation and optimization used by density-based topology optimization and porous infill optimization by adopting a multi-scale strategy:

Homogenization-based topology optimization. During the initial optimization, a coarse-scale representation is tuned to approach the optimal distribution of material across a structure. This structure doesn’t represent the exact material layout but rather provides a set of specifications to guide the optimal material layout.

Dehomogenization. Once the optimized specifications are found, dehomogenization is the process of converting coarse, homogenized results into detailed, fine-scaled structures. This involves creating actual geometric elements (trusses, lattices, microstructures) realizing the material properties and orientations suggested by the homogenized result.

Homogenization-based topology optimization provides an orthotropic direction field as the optimized specifications. Dehomogenization extracts a conforming lattice structure with edges aligning with the direction field, and aspect ratios or sizes conveying the associated properties of the corresponding directions. The optimal directions are given by the principal stress directions of the homogenization-based structure layout. SGLDBench directly feeds the stress field in the solid domain to the dehomogenization stage, where it is used to generate a stress-aligned lattice structure. The cell sizes of the generated structure can either adapt to the local von Mises stresses or remain nearly constant. In Fig. 9, the adaptive lattice structure is compared to the one with a uniform cell size. Both infills are stress-aligned with the same material consumption, yet one can easily see that the adaptive lattice structure gives significantly improved stiffness.

The conforming lattice structure circumvents the intersection issue of PSL-guided infills by relaxing the requirement of strictly following the principal stress directions. The method builds upon

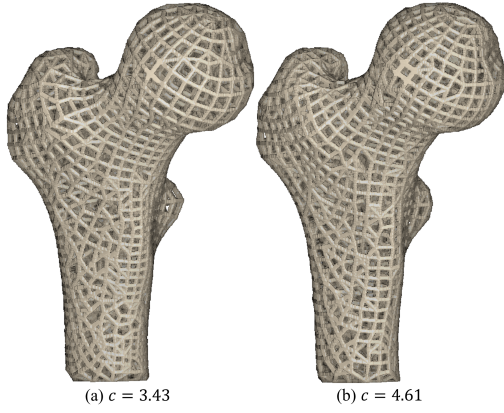


Fig. 9. Conforming lattice structure. (a) Non-uniform infill layout according to principal stress amplitudes. (b) Uniform layout.

the field-aligned hex-dominant meshing approach by Gao *et al.* [10], which uses an orthogonal frame field and aligns the edges of a hexahedral mesh with this field. The frame field is replaced with the field of principal stress directions, and the mechanical anisotropy is considered in the field-aligned parameterization process.

Due to the existence of degenerate points and regions in a stress field, however, for all but simple fields, it is impossible to compute a conforming hexahedral mesh. Conforming lattice structure addresses this limitation by pursuing a local smoothing strategy. The key idea is to exploit the rotational symmetry of principal stress directions to generate a smoothed direction field from which a conforming hexahedral mesh can be constructed. From this field, a position field whose gradient aligns with the adjusted stress directions is computed. Finally, by using the smoothed direction field and the position field in combination, the method constructs a graph structure and extracts the final mesh from this structure. Conforming lattice structure aim at generating a regular mesh, at the same time maintaining the divergence/convergence properties of the underlying stress field. This is achieved by introducing irregular vertex connections in the final structure, resulting in an edge-graph structure.

3.3.6 Volumetric Michell trusses

Volumetric Michell Trusses compute a stress-aligned hexahedral lattice using a parametric approach to align truss elements with the principal directions of the stress field. This method involves two key steps:

Frame Field Smoothing. The algorithm first applies an FEA to compute the stress tensor field, followed by a frame field generation aligned with the principal stress directions. However, to achieve a global parametric structure, this step smooths out tensor field singularities, sacrificing local alignment near degenerate points for overall global consistency. To address this, the method uses Loubignac iterations [54] to smooth out the discontinuous stress field. This iterative method adjusts the stress field to ensure that it becomes continuous across element boundaries, thereby allowing for smoother and more uniform alignment in subsequent steps. Therefore, a smoothness energy function that penalizes sharp changes of frame directions is minimized. This optimization enables a globally smooth frame field that approximates the original stress directions.

Tracing Integer Isolines. After smoothing, integer isolines of the volumetric texture parameterization are traced. This step maps the truss nodes to integer points of the parameterization, yielding the

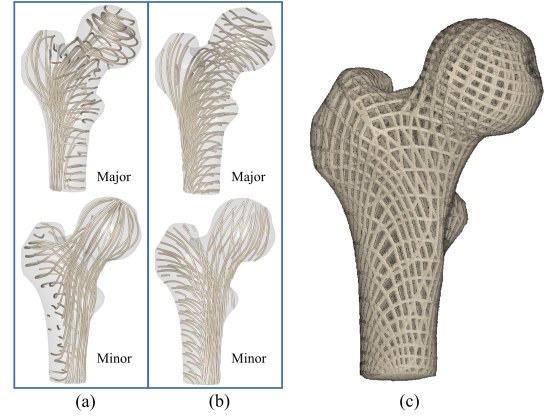


Fig. 10. Volumetric Michell trusses. (a) PSLs in the loaded solid domain. (b) PSLs in the smoothed stress field. (c) Resulting design.

geometry for the extracted graph structure. Its connectivity follows from the nodes' adjacency in the grid. To ensure flexibility, the method allows scaling of the parameterization via a user-defined resolution parameter ρ , which controls the density of the truss structure.

Due to the applied smoothing of the initial stress field, volumetric Michell trusses produce a regular hexahedral lattice structure with improved continuity of load transmissions. Fig. 10 compares an initial stress field to the smoothed frame field that is used to generate an infill with this method. The smoothing, on the other hand, can significantly modify the initial stress field, so that the resulting stiffness of a design can also deviate significantly from the optimum.

3.4 Infill Voxelization

While topology optimization and porous infill compute a binary material field on a 3D voxel grid, the other methods compute a 3D lattice structure composed of edges and nodes. To enable a meaningful comparison of the structural properties of all approaches, SGLDBench voxelizes these structures into a voxel grid. The grid resolution is selected automatically to represent edges with a minimum required voxels. SGLDBench computes for each edge the intersected voxels via the DDA line drawing algorithm [55]. These voxels are set to solid. Edges are thickened by setting for all these voxels their 26 neighboring voxels to solid.

For all edge-based infill strategies, the material budget and the targeted edge thickness are prescribed. The methods are then conducted in a dichotomy manner to find the settings that matches closely the design specifications, i.e., the design process is run multiple times to find the design that matches the material consumption under the edge thickness constraint.

3.5 Layout Analysis and Comparison

Once a 3D material design is computed, SGLDBench uses the linear elasticity solver to compute the compliance of the design. Irrespectively of the used design strategy, this requires a final FEA to simulate the stress field.

The user can view the meshes and graph structures generated by Voronoi infill, PSL-guided infill, conforming lattice structure and volumetric Michell trusses with MATLAB's mesh viewing operations. The material fields generated with density-based topology optimization and porous infill optimization can be visualized with MATLAB's functionality to render isosurfaces in 3D scalar fields,

providing immediate feedback of the geometry and thickness of the produced structures.

Over that, SGLDBench provides an advanced WebGL-based volume visualization module to perform isosurface rendering and a stress-based comparative analysis of designs. Iso-surfaces in a 3D material field are rendered via ray-casting, with screen-space ambient occlusion for improved perception of the 3D structure of a design. All surface visualizations in this paper have been produced with this option.

In addition, SGLDBench’s visualization module conveys the differences between the principal stress directions in the solid design and the computed infill design. SGLDBench computes the stress field using the initial boundary conditions, and then generates an auxiliary grid in which each voxel stores a single deviation measure. Based on the ordering of the absolute values of the principal stresses in the initial solid and the infill, the measure indicates the deviation of the stress directions corresponding to the principal stresses with maximum absolute value. The resulting scalar field is visualized via direct volume rendering. SGLDBench uses a transfer function that maps directional deviations linearly to colors ranging from white (low deviation) over light brown (medium deviation) to dark brown (high deviation). Opacity is linearly increased from low to high deviations, yet it starts at a base of 0.3 to also make low deviation regions visible.

4 EXPERIMENTS

We demonstrate the use of SGLDBench to generate and analyze lightweight designs for different models and boundary conditions. We use a model of a human femur (*Bone*), a machine part that is often seen in engineering applications (*Part*), and *Cantilever*, a popular benchmark model in topology optimization (see Figs. 2 and 11). All models are initially given as triangle meshes.

All experiments are performed on a desktop computer equipped with an Intel CPU (6-core Xeon W2235), 64 GB of RAM, and an NVIDIA RTX 2070 GPU with 8 GB of video memory. We select a mid-end architecture on purpose to demonstrate SGLDBench’s capabilities even on affordable hardware. The main memory limits the maximum number of simulation elements that can be used by SGLDBench to roughly 160 million elements when simulating a 3D stress field. For *Cantilever* at a voxel grid resolution of $860 \times 430 \times 430$ (159 million elements), SGLDBench solves the FEA linear system on the CPU in roughly 30 minutes, with 41 solver iterations until reaching the convergence threshold of 1.0×10^{-3} .

Topology optimization and porous infill optimization require additional memory for updating the material distribution using numerical optimization. SGLDBench performs these optimizations with about 130 million simulation elements. This corresponds to a $800 \times 400 \times 400$ simulation grid with 386 million degrees of freedom. SGLDBench requires about 45 minutes and 67 minutes, respectively, per optimization iteration of topology optimization and porous infill optimization. The results in Fig. 11 are generated by topology optimization and porous infill optimization with respectively 30 and 280 optimization iterations. In comparison to an optimized OpenMP CPU implementation of topology optimization [37], SGLDBench is only about a factor of 1.6 slower when reproducing the same cantilever model with equal resolution of $640 \times 320 \times 320$ on a similar computing architecture, i.e., a 48-core Xeon architecture. This demonstrates the efficiency of the MATLAB computing environment in combination with SGLDBench’s element-wise computation structure.

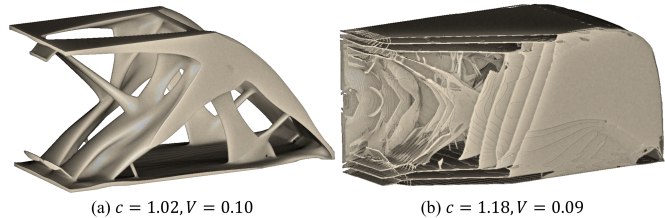


Fig. 11. Material fields generated with topology optimization (a) and porous infill optimization (b) for *Cantilever* using a voxel grid of resolution $800 \times 400 \times 400$. The left face of the cubic design domain is fixed, and a downward force is uniformly applied at the bottom-right edge.

A one-to-one CUDA implementation of the solver by Wu *et al.* [31] on the RTX 2070 GPU can simulate up to 45 million elements before running out of GPU memory. For this number of elements, the GPU implementation needs 91 seconds to solve the FEA linear system. SGLDBench requires 610 seconds for the same setting, showing roughly a 7x reduction of the performance compared to the optimized GPU solver. For the used GPU this is a reasonable reduction, and slightly better than commonly reported when GPU and CPU implementations of similar problems are compared.

All designs for *Bone* in Fig. 2 are generated with a $384 \times 256 \times 512$ voxel grid, corresponding to 9.8 million simulation elements. Topology optimization and porous infill optimization, respectively, generate the infill in 1.5 hours and 15.1 hours. Porous infill requires a significantly higher number of optimization iterations and additional computations to enforce the local volume constraint. Due to the high geometric complexity of porous infills, generating these infill also requires a higher number of iterations for solving the linear FEA system in each optimization iteration.

SGLDBench needs about 10 minutes to generate the Voronoi infill and the PSL-guided infill. About half of the time is required to simulate the 3D stress field in the initial solid domain. With this stress field, executing the external codes to generate the conforming lattice infill and the MATLAB code to generate the volumetric Michell truss requires 5 minutes and 4.5 hours, respectively. Slightly less than one half of the execution time of the latter is used for smoothing the original stress field.

4.1 Material Use as a Modelling Parameter

To compare the response of different design methods to changes in the consumed material, we repeat all experiments shown in Fig. 2 with reduced volume fraction. Instead of a volume fraction of 0.4, SGLDBench now uses a low volume fraction of roughly 0.2 to enforce finer and lesser support structures. For all approaches generating a graph structure, the thickness of the voxelized edges is kept constant. The results are shown in Fig. 12, indicating increasing sparseness of all designs, at decreasing stiffness and with vastly different topologies. Topology optimization and porous infill do not require any modification of their simulation parameters, yet the entire optimization needs to be rerun to generate the results. All other approaches can use the stress field in the initial solid domain, and need to rerun only those parts generating the graph structure from it.

In particular, with a lower material budget the PSL-guided infill shows surprisingly good relative performance, since it uses the material to generate support structures along the most dominant stress directions. While with the 2D motivational example the conforming lattice infill has higher stiffness than the Voronoi infill

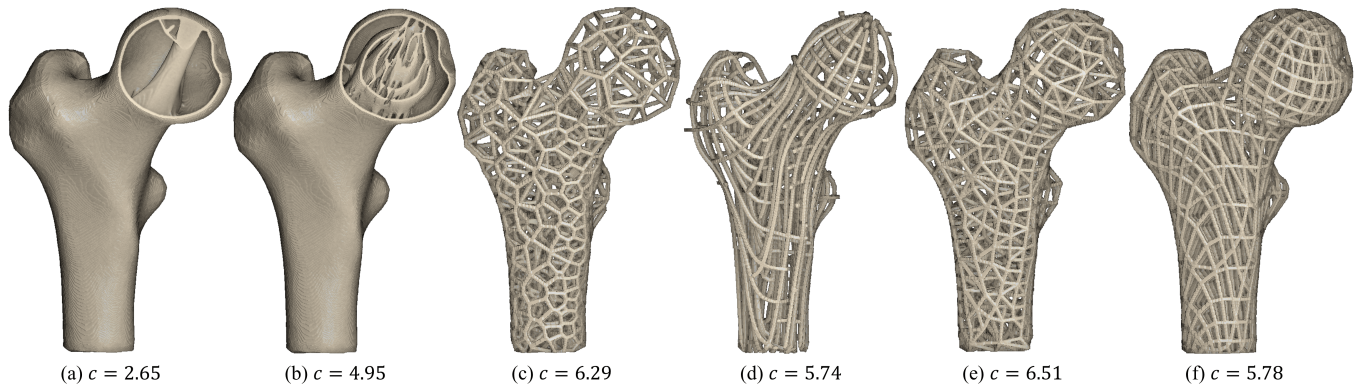


Fig. 12. (a) Density-based topology optimization. (b) Porous infill optimization. (c) Voronoi infill. (d) PSL-guided material layout. (e) Conforming lattice structures. (f) Volumetric Michell trusses. All infills consume roughly the same volume fraction of 0.22.

and the volumetric Michell trusses (see Fig. 1), with *Bone* the mechanical properties have reversed. One reason might be that the resolution of the conforming lattice is too low, causing many edges of the graph structure to be misaligned with the dominant stress directions. In addition to the alignment of edges with the major stress directions, adaptive porosity also makes an important contribution to reducing compliance. I.e., in regions of high stresses, more material should be accumulated to resist the strain. This might be one reason for the rather moderate stiffness of the Voronoi infill, which cannot accumulate more material in regions of high stress due to the low material budget. Furthermore, the Voronoi infill, per construction, does not align with the dominant stress directions.

Since the stress field in *Bone* is rather simple and does not contain many degeneracies, most features can be well maintained by the Michell trusses. This, however, changes with *Cantilever*, see Fig. 15. Since the smoothed stress field of *Cantilever* shows significant differences to the initial field, many infill edges deviate strongly from the initial stress directions. This results in lower stiffness compared to the other alternatives.

4.2 Infill Resolution and Compliance

To shed light on the relationship between compliance, volume fraction, and geometric infill resolution, SGLDBench is used to evaluate the stiffness of high-resolution lattice infills for *Bone*. The infills are computed with SGLDBench, but they can also be generated with any other approach that produces an infill as a tetrahedral/hexahedral grid or an edge-graph. In the latter case, the infill is uploaded to SGLDBench and voxelized into a voxel grid. The volume fraction, the edge thickness, and the voxel grid resolution are defined by the user. Finally, SGLDBench computes the infill’s compliance using one FEA iteration.

In Fig. 13, a voxelized conforming lattice infill and a Voronoi infill with 136,877 and 396,458 edges, respectively, are shown. SGLDBench generates the infills using the same boundary conditions as in Figs 2 and 12. SGLDBench voxelizes the infills into a $848 \times 576 \times 1200$ voxel grid and builds a finite element model from it. The voxelized versions of the infills are visualized using SGLDBench’s WebGL visualization module with isosurface ray-casting and ambient occlusions. For computing the compliance of the voxel models, about 380 million degrees of freedom are solved. SGLDBench does this in roughly 45 minutes. Interestingly, with the same material budget, the stiffness doesn’t seem to depend on the geometric details of the infills, as indicated by Fig. 2.

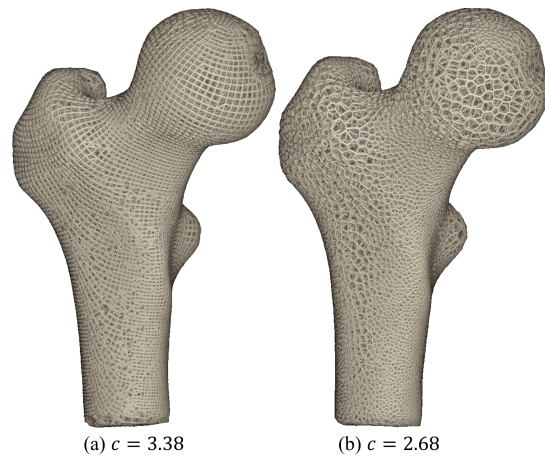


Fig. 13. High resolution conforming lattice infill (a) and Voronoi infill (b), using the same boundary conditions and material budget as in Fig. 2.

4.3 Infill Geometry

Given the different compliances of different types of infills for the same object and load condition, we use SGLDBench to shed light on the major causes of these differences. Therefore, we compare the interior structure of the graph-based infill approaches, as demonstrated with *Bone* in Fig. 14. A clip plane is used to reveal some interior parts of the PSL-guided infill, the conforming lattice structure and the volumetric Michell trusses.

The PSL-guided infill serves as a reference that shows the major load transmission pathways. The edges of the conforming lattice structure align with the PSLs overall. In regions where the curvature of the PSLs changes significantly (see the inset in Fig. 14), however, the lattice loses its geometric regularity. The degeneracies in the stress field where the principal stress directions flip seem to indicate these irregularities. Volumetric Michell trusses, on the other hand, exhibit a very regular geometric structure, yet it shows less alignment with the original stress directions. This is because the original stress field is smoothed, which changes the stress field globally and removes in particular unwanted degeneracies.

The visualization of the 3D conforming lattice structure indicates a number of stitching edges in the interior that do not align with any of the dominant stress directions. The number of longer sequences of edges that follow consistently one of the PSL trajectories is lower compared to the PSL-guided infill and the volumetric Michell trusses. The reason for this behavior might be that the 3D conforming lattice structure uses too much material to

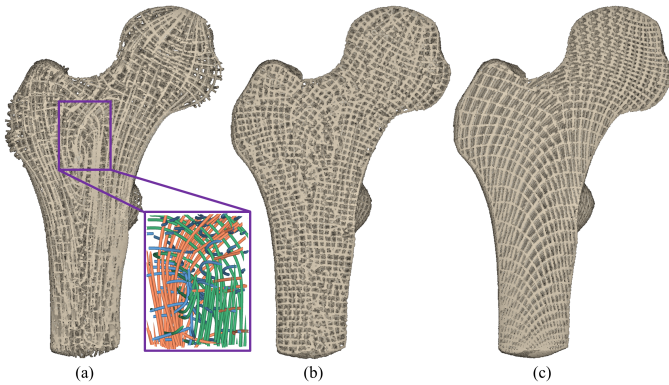


Fig. 14. From (a) to (c), via a clip plane the interior of the PSL-guided lattice infill, the conforming lattice structure and volumetric Michell trusses are revealed. The closeup view shows the PSLs in the selected region, with the major, medium, and minor PSLs, respectively, shown in orange, green and blue.

obtain a consistent edge-graph rather than accounting for stiffness. Oscillating load paths, i.e., edge sequences, might result in less effective load transitions and reduced stiffness.

4.4 Reproducing Stresses in the Solid Domain

With *Part* shown in Fig. 15, SGLDBench is used to analyze how well different designs reproduce the stress directions in the initial solid configuration. In this way, users can, for instance, analyze whether the transmission of forces through tension and compression is along the same load paths as in the initial solid. Since an infill design can, in principle, transmit forces along the most efficient load paths in the solid design or use different paths, revealing relationships between compliance and reproduction of stress directions can give further hints on how to improve infill designs.

Fig. 16 shows visualizations of the auxiliary grids that are computed for each infill. Direct volume rendering with the color and opacity transfer functions described in Sec. 3.4 is used to emphasize regions with high deviation in brown. Topology optimization generates an infill that in many parts reproduces the major stress directions in the solid under load. However, also some regions with major deviations can be seen, especially some thin structures and structures close to the fixed elements where stresses are highest. The same holds for porous infill, yet overall it shows slightly higher deviations that are spread over the entire domain due to the more space-filling distribution of material.

It is clear that the stress deviations are highest in the Voronoi infill, because the initial stress directions are not considered in the edge-graph layout. The stress deviations are low when edges cover boundary elements, since these elements are considered in the stress analysis of the solid object and the infill. The material in the PSL-guided infill is distributed along the principal stress directions, and, thus, stresses are well aligned with these directions. However, as also seen in Fig. 3, at the boundaries of the voxelized edges the alignment is less accurate. This is due to inaccuracies in the stress simulation using the discretized line structures, a property that holds for all graph-based approaches when using the voxelized structures for the compliance analysis. Furthermore, since all graph-based infills contain many edges along the two stress directions not corresponding to the direction with the maximum absolute stress value, a high directional deviation can occur along these edges.

The deviation maps of the conforming lattice structure and the Michell trusses are very similar, showing the same low deviation patterns in the boundary region as the Voronoi infill. In both infills there is still a considerable number of voxels with significantly different dominant stress direction than the solid object.

In the supplementary material, we further demonstrate the usability of SGLDBench with additional datasets, which will be made available together with the code repository.

5 CONCLUSION AND OUTLOOK

SGLDBench is a benchmark suite for stiff lightweight design simulation and analysis, with special emphasis on high-resolution 3D designs. It supports the computation of six different types of designs, using methods spanning the wide spectrum from purely stiffness-based optimization to geometry-aware infill generation. SGLDBench enables users to create different types of designs at different resolutions and with different material consumptions, and to assess their mechanical and geometric properties. Direct volume rendering with ambient occlusion is used to improve the visual perception of high-resolution 3D designs. SGLDBench visualizes the deviations between stress directions in the initial solid object and a generated design to reveal relationships between stiffness, geometric properties, and stress replication.

SGLDBench can be used to compute individual designs with specific boundary conditions. New design strategies can be integrated into the publically available code basis. Over that, SGLDBench can be used to create new types of designs by combining existing design strategies. For instance, the material field of an optimal design can be computed via topology optimization and downloaded to extract the design boundary as an isosurface in this field. This surface can then be uploaded to SGLDBench to compute an infill that is restricted to the surface's interior. An example is shown in the supplemental material.

By using SGLDBench's functionality, a number of interesting properties of existing design strategies have been revealed, guiding toward new research directions in lightweight design: Why is the mechanical performance of conforming lattice structures below expectation in 3D domains? What is the role of adaptive porosity in achieving high stiffness? What is the interplay between truss thickness, cell size, and stiffness in lattice infills? How does an optimal smoothing operator for a tensor field look so that the stiffness deviation is minimized, e.g., so that forces are still transmitted along the most efficient load paths? How does a Voronoi infill perform if further constraints on the edges regarding stress reproduction are enforced? SGLDBench supports researchers in finding answers to these questions and developing improved design strategies regarding different objectives.

ACKNOWLEDGMENTS

This work was supported by the German Research Foundation (DFG) under grant number WE 2754/10-1. Several open-source projects are used when developing SGLDBench, including the volumetric Michell structure [11], conforming lattice structures [50], the tetrahedral mesh generator *TetGen* [56], and the voxelization functions [36], the MMA implementations [40], [57]. Hereby, We sincerely acknowledge the generosity of the authors for making their code publicly available.

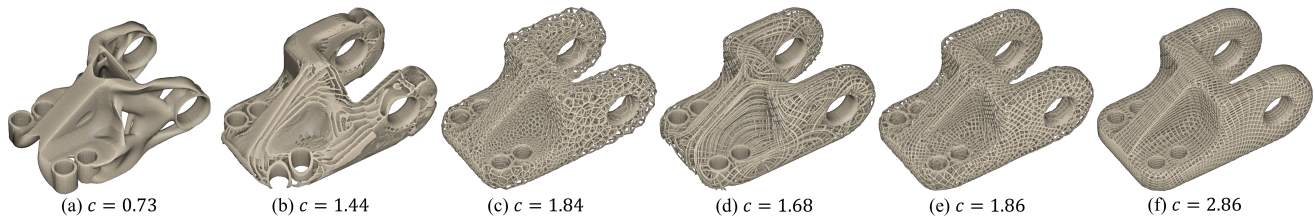


Fig. 15. (a) Density-based topology optimization. (b) Porous infill optimization. (c) Voronoi infill. (d) PSL-guided infill. (e) Conforming lattice structures. (f) Volumetric Michell trusses. All infills consume roughly the same volume fraction of 0.3.

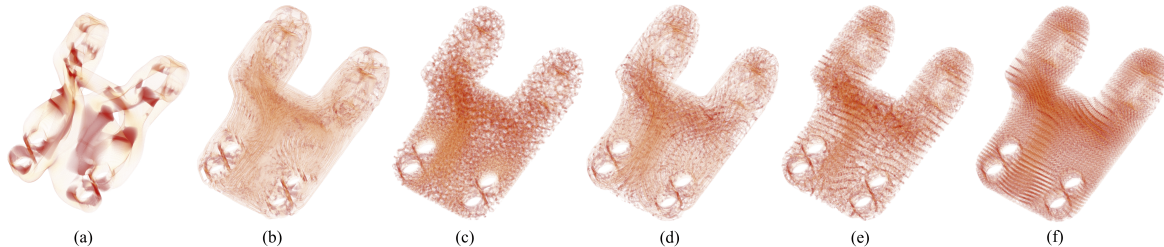
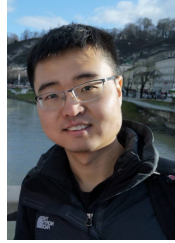


Fig. 16. Stress-to-stress alignment. (a) Topology optimization. (b) Porous infill optimization. (c) Voronoi infill. (d) PSL-guided infill. (e) Conforming lattice. (f) Volumetric Michell trusses.

REFERENCES

- [1] M. P. Bendsøe, "Optimal shape design as a material distribution problem," *Structural Optimization*, vol. 1, no. 4, pp. 193–202, 1989.
- [2] G. Allaire, F. Jouve, and A.-M. Toader, "Structural optimization using sensitivity analysis and a level-set method," *Journal of Computational Physics*, vol. 194, no. 1, pp. 363–393, 2004.
- [3] J. Wu, O. Sigmund, and J. P. Groen, "Topology optimization of multi-scale structures: a review," *Structural and Multidisciplinary Optimization*, pp. 1–26, 2021.
- [4] P. Pedersen, "On optimal orientation of orthotropic materials," *Structural optimization*, vol. 1, no. 2, pp. 101–106, 1989.
- [5] A. G. M. Michell, "Lviii. the limits of economy of material in frame-structures," *The London, Edinburgh, and Dublin Philosophical Magazine and Journal of Science*, vol. 8, no. 47, pp. 589–597, 1904.
- [6] O. Sigmund, "Materials with prescribed constitutive parameters: an inverse homogenization problem," *International Journal of Solids and Structures*, vol. 31, no. 17, pp. 2313–2329, 1994.
- [7] J. Wu, N. Aage, R. Westermann, and O. Sigmund, "Infill optimization for additive manufacturing – approaching bone-like porous structures," *IEEE Transactions on Visualization and Computer Graphics*, vol. 24, no. 2, pp. 1127–1140, 2018.
- [8] L. Lu, A. Sharf, H. Zhao, Y. Wei, Q. Fan, X. Chen, Y. Savoye, C. Tu, D. Cohen-Or, and B. Chen, "Build-to-last: Strength to weight 3d printed objects," *ACM Transactions on Graphics (TOG)*, vol. 33, no. 4, pp. 1–10, 2014.
- [9] J. Wang, J. Wu, and R. Westermann, "Stress trajectory guided structural design and topology optimization," in *International Design Engineering Technical Conferences and Computers and Information in Engineering Conference*, vol. 1. American Society of Mechanical Engineers, 2022, p. 1.
- [10] X. Gao, W. Jakob, M. Tarini, and D. Panozzo, "Robust hex-dominant mesh generation using field-guided polyhedral agglomeration," *ACM Transactions on Graphics (TOG)*, vol. 36, no. 4, pp. 1–13, 2017.
- [11] R. Arora, A. Jacobson, T. R. Langlois, Y. Huang, C. Mueller, W. Matusik, A. Shamir, K. Singh, and D. I. Levin, "Volumetric michell trusses for parametric design & fabrication," in *Proceedings of the ACM Symposium on Computational Fabrication*. ACM, 2019, pp. 1–13.
- [12] J. Plocher and A. Panesar, "Review on design and structural optimisation in additive manufacturing: Towards next-generation lightweight structures," *Materials & Design*, vol. 183, p. 108164, 2019.
- [13] Z. Jihong, Z. Han, W. Chuang, Z. Lu, Y. Shangqin, and W. Zhang, "A review of topology optimization for additive manufacturing: Status and challenges," *Chinese Journal of Aeronautics*, vol. 34, no. 1, pp. 91–110, 2021.
- [14] A. Bacciaglia, A. Ceruti, and A. Liverani, "A systematic review of voxelization method in additive manufacturing," *Mechanics & Industry*, vol. 20, no. 6, p. 630, 2019.
- [15] T. Delmarcelle and L. Hesselink, "The topology of symmetric, second-order tensor fields," in *Proceedings Visualization'94*. IEEE, 1994, pp. 140–147.
- [16] J. Wang, J. Wu, and R. Westermann, "A globally conforming lattice structure for 2D stress tensor visualization," *Computer Graphics Forum*, vol. 39, no. 3, pp. 417–427, 2020.
- [17] C. Hergl, C. Blecha, V. Kretschmar, F. Raith, F. Günther, M. Stommel, J. Jankowai, I. Hotz, T. Nagel, and G. Scheuermann, "Visualization of tensor fields in mechanics," in *Computer Graphics Forum*, vol. 40, no. 6. Wiley Online Library, 2021, pp. 135–161.
- [18] S.-H. Hung, Y. Zhang, and E. Zhang, "Global topology of 3d symmetric tensor fields," *IEEE Transactions on Visualization and Computer Graphics*, 2023.
- [19] F. C. Stutz, J. P. Groen, O. Sigmund, and J. A. Barentzen, "Singularity aware de-homogenization for high-resolution topology optimized structures," *Structural and Multidisciplinary Optimization*, aug 2020.
- [20] S. Rojas-Labanda and M. Stolpe, "Benchmarking optimization solvers for structural topology optimization," *Structural and Multidisciplinary Optimization*, vol. 52, no. 3, pp. 527–547, 2015.
- [21] S. I. Valdez, S. Botello, M. A. Ochoa, J. L. Marroquín, and V. Cardoso, "Topology optimization benchmarks in 2d: results for minimum compliance and minimum volume in planar stress problems," *Archives of Computational Methods in Engineering*, vol. 24, pp. 803–839, 2017.
- [22] O. Sigmund, "On benchmarking and good scientific practise in topology optimization," *Structural and Multidisciplinary Optimization*, vol. 65, no. 11, p. 315, 2022.
- [23] B. Pernet, J. K. Nagel, and H. Zhang, "Compressive strength assessment of 3d printing infill patterns," *Procedia CIRP*, vol. 105, pp. 682–687, 2022, the 29th CIRP Conference on Life Cycle Engineering, April 4 – 6, 2022, Leuven, Belgium. [Online]. Available: <https://www.sciencedirect.com/science/article/pii/S2212827122001159>
- [24] J. R. Martins and A. B. Lambe, "Multidisciplinary design optimization: a survey of architectures," *AIAA journal*, vol. 51, no. 9, pp. 2049–2075, 2013.
- [25] F. Tamburrino, S. Graziosi, and M. Bordegoni, "The design process of additively manufactured mesoscale lattice structures: a review," *Journal of Computing and Information Science in Engineering*, vol. 18, no. 4, p. 040801, 2018.
- [26] C. Pan, Y. Han, and J. Lu, "Design and optimization of lattice structures: A review," *Applied Sciences*, vol. 10, no. 18, p. 6374, 2020.
- [27] A. Seharang, A. H. Azman, and S. Abdullah, "A review on integration of lightweight gradient lattice structures in additive manufacturing parts," *Advances in Mechanical Engineering*, vol. 12, no. 6, p. 1687814020916951, 2020.
- [28] T. Maconachie, M. Leary, B. Lozanovski, X. Zhang, M. Qian, O. Faruque, and M. Brandt, "SLM lattice structures: Properties, performance, applications and challenges," *Materials & Design*, vol. 183, p. 108137, 2019.
- [29] C. Zhang, J. Liu, Z. Yuan, S. Xu, B. Zou, L. Li, and Y. Ma, "A novel lattice structure topology optimization method with extreme anisotropic

- lattice properties,” *Journal of Computational Design and Engineering*, vol. 8, no. 5, pp. 1367–1390, 2021.
- [30] C. Dick, J. Georgii, and R. Westermann, “A real-time multigrid finite hexahedra method for elasticity simulation using cuda,” *Simulation Modelling Practice and Theory*, vol. 19, no. 2, pp. 801–816, 2011.
- [31] J. Wu, C. Dick, and R. Westermann, “A system for high-resolution topology optimization,” *IEEE transactions on visualization and computer graphics*, vol. 22, no. 3, pp. 1195–1208, 2015.
- [32] H. Liu, Y. Hu, B. Zhu, W. Matusik, and E. Sifakis, “Narrow-band topology optimization on a sparsely populated grid,” *ACM Transactions on Graphics (TOG)*, vol. 37, no. 6, pp. 1–14, 2018.
- [33] N. Aage, E. Andreassen, B. S. Lazarov, and O. Sigmund, “Giga-voxel computational morphogenesis for structural design,” *Nature*, vol. 550, no. 7674, pp. 84–86, 2017.
- [34] O. Sigmund, “A 99 line topology optimization code written in Matlab,” *Structural and multidisciplinary optimization*, vol. 21, no. 2, pp. 120–127, 2001.
- [35] J. Wang, C. Neuhauser, J. Wu, X. Gao, and R. Westermann, “3D-TSV: The 3D trajectory-based stress visualizer,” *Advances in Engineering Software*, vol. 170, p. 103144, 2022.
- [36] A. H. Aitkenhead. (2013) Mesh voxelisation. [Online]. Available: <https://www.mathworks.com/matlabcentral/fileexchange/27390-mesh-voxelisation>
- [37] E. A. Träff, A. Rydahl, S. Karlsson, O. Sigmund, and N. Aage, “Simple and efficient gpu accelerated topology optimisation: Codes and applications,” *Computer Methods in Applied Mechanics and Engineering*, vol. 410, p. 116043, 2023.
- [38] K. Liu and A. Tovar, “An efficient 3d topology optimization code written in matlab,” *Structural and multidisciplinary optimization*, vol. 50, pp. 1175–1196, 2014.
- [39] F. Wang, B. S. Lazarov, and O. Sigmund, “On projection methods, convergence and robust formulations in topology optimization,” *Structural and Multidisciplinary Optimization*, vol. 43, no. 6, pp. 767–784, 2011.
- [40] K. Svanberg, “The method of moving asymptotes—a new method for structural optimization,” *International journal for numerical methods in engineering*, vol. 24, no. 2, pp. 359–373, 1987.
- [41] J. Martínez, J. Dumas, and S. Lefebvre, “Procedural voronoi foams for additive manufacturing,” *ACM Transactions on Graphics (TOG)*, vol. 35, no. 4, pp. 1–12, 2016.
- [42] J. Martínez, H. Song, J. Dumas, and S. Lefebvre, “Orthotropic k-nearest foams for additive manufacturing,” *ACM Trans. Graph.*, vol. 36, no. 4, Jul. 2017. [Online]. Available: <https://doi.org/10.1145/3072959.3073638>
- [43] A. Jacobson, L. Kavan, and O. Sorkine-Hornung, “Robust inside-outside segmentation using generalized winding numbers,” *ACM Transactions on Graphics (TOG)*, vol. 32, no. 4, pp. 1–12, 2013.
- [44] I. E. Sutherland and G. W. Hodgman, “Reentrant polygon clipping,” *Communications of the ACM*, vol. 17, no. 1, pp. 32–42, 1974.
- [45] H. Edelsbrunner and N. R. Shah, “Triangulating topological spaces,” in *Proceedings of the tenth annual symposium on Computational geometry*, 1994, pp. 285–292.
- [46] J. Martínez, S. Hornus, H. Song, and S. Lefebvre, “Polyhedral voronoi diagrams for additive manufacturing,” *ACM Transactions on Graphics (TOG)*, vol. 37, no. 4, pp. 1–15, 2018.
- [47] P. Virtanen, R. Gommers, T. E. Oliphant, M. Haberland, T. Reddy, D. Cournapeau, E. Burovski, P. Peterson, W. Weckesser, J. Bright *et al.*, “Scipy 1.0: fundamental algorithms for scientific computing in python,” *Nature methods*, vol. 17, no. 3, pp. 261–272, 2020.
- [48] C. B. Barber, D. P. Dobkin, and H. Huhdanpaa, “The quickhull algorithm for convex hulls,” *ACM Transactions on Mathematical Software (TOMS)*, vol. 22, no. 4, pp. 469–483, 1996.
- [49] T.-H. Kwok, Y. Li, and Y. Chen, “A structural topology design method based on principal stress line,” *Computer-Aided Design*, vol. 80, pp. 19–31, 2016.
- [50] J. Wu, W. Wang, and X. Gao, “Design and optimization of conforming lattice structures,” *IEEE Transactions on Visualization and Computer Graphics*, vol. 27, no. 1, pp. 43–56, 2021.
- [51] O. Pantz and K. Trabelsi, “A post-treatment of the homogenization method for shape optimization,” *SIAM Journal on Control and Optimization*, vol. 47, no. 3, pp. 1380–1398, 2008.
- [52] J. P. Groen and O. Sigmund, “Homogenization-based topology optimization for high-resolution manufacturable microstructures,” *International Journal for Numerical Methods in Engineering*, vol. 113, no. 8, pp. 1148–1163, 2018.
- [53] G. Allaire, P. Geoffroy-Donders, and O. Pantz, “Topology optimization of modulated and oriented periodic microstructures by the homogenization method,” *Computers & Mathematics with Applications*, vol. 78, no. 7, pp. 2197–2229, 2019.
- [54] G. Loubignac, G. Cantin, and G. Touzot, “Continuous stress fields in finite element analysis,” *AIAA journal*, vol. 15, no. 11, pp. 1645–1647, 1977.
- [55] J. Amanatides, A. Woo *et al.*, “A fast voxel traversal algorithm for ray tracing,” in *Eurographics*, vol. 87, no. 3. Citeseer, 1987, pp. 3–10.
- [56] S. Hang, “Tetgen, a delaunay-based quality tetrahedral mesh generator,” *ACM Trans. Math. Softw.*, vol. 41, no. 2, p. 11, 2015.
- [57] N. Aage and B. S. Lazarov, “Parallel framework for topology optimization using the method of moving asymptotes,” *Structural and multidisciplinary optimization*, vol. 47, no. 4, pp. 493–505, 2013.



Junpeng Wang is a Post-doc in the Computer Graphics and Visualization Group at Technical University of Munich, Germany. He obtained his PhD from the same group in 2023. His research interests range from scientific visualization to computational design, with a special focus on lightweight structure design and optimization.



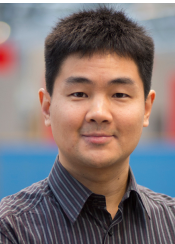
Dennis R. Bukenberger is a postdoc in the Computer Graphics and Visualization Group at the Technical University of Munich, Germany. Before this, he was a postdoc at the Technical University of Dortmund. He obtained his PhD at the University of Tübingen in 2021. His research interests include meshing algorithms, Voronoi diagrams, geometry processing & sustainable design engineering.



Simon Niedermayr is a PhD candidate at the Computer Graphics and Visualization Group at the Technical University of Munich (TUM). He received his Master's degrees in computer science from TUM in 2022. His research interests include differentiable rendering, real-time rendering and high performance GPGPU programming.



Christoph Neuhauser is a PhD candidate at the Computer Graphics and Visualization Group at the Technical University of Munich (TUM). He received his Bachelor's and Master's degrees in computer science from TUM in 2019 and 2020. Major interests in research comprise scientific visualization and real-time rendering.



Jun Wu is an associate professor at the Department of Sustainable Design Engineering, Delft University of Technology. Before this, he was a Marie Curie postdoc fellow at the Department of Mechanical Engineering, Technical University of Denmark. He obtained a PhD in Computer Science in 2015 from TUM, and a PhD in Mechanical Engineering in 2012 from Beihang University, Beijing. His research is focused on computational design and digital fabrication, with an emphasis on topology optimization.



Rüdiger Westermann is a full professor for Computer Science in the TUM School of Computation, Information and Technology. He is the head of Computer Graphics and Visualization group. His research interests include scalable data visualization and simulation algorithms, GPU computing, topology optimization, neural representations for computer graphics and visualization, as well as real-time and photorealistic rendering.